The EMBO Journal (2008) 27, 1747–1757 | © 2008 European Molecular Biology Organization | All Rights Reserved 0261-4189/08
www.embojournal.org

THE EMBO JOURNAL

pVHL and PTEN tumour suppressor proteins cooperatively suppress kidney cyst formation

Ian J Frew[1], Claudio R Thoma[1], Strahil Georgiev[1], Andrea Minola[1], Manuela Hitz[1], Matteo Montani[1,2], Holger Moch[2] and Wilhelm Krek[1,*]

[1]Institute of Cell Biology, ETH Zurich, Zurich, Switzerland and [2]Institute of Clinical Pathology, University Hospital Zurich, Zurich, Switzerland

In patients with von Hippel–Lindau (VHL) disease, renal cysts and clear cell renal cell carcinoma (ccRCC) arise from renal tubular epithelial cells containing biallelic inactivation of the *VHL* tumour suppressor gene. However, it is presumed that formation of renal cysts and their conversion to ccRCC involve additional genetic changes at other loci. Here, we show that cystic lesions in the kidneys of patients with VHL disease also demonstrate activation of the phosphatidylinositol-3-kinase (PI3K) pathway. Strikingly, combined conditional inactivation of *Vhlh* and the *Pten* tumour suppressor gene, which normally antagonises PI3K signalling, in the mouse kidney, elicits cyst formation after short latency, whereas inactivation of either tumour suppressor gene alone failed to produce such a phenotype. Interestingly, cells lining these cysts frequently lack a primary cilium, a microtubule-based cellular antenna important for suppression of uncontrolled kidney epithelial cell proliferation and cyst formation. Our results support a model in which the PTEN tumour suppressor protein cooperates with pVHL to suppress cyst development in the kidney.

The EMBO Journal (2008) **27,** 1747–1757. doi:10.1038/emboj.2008.96; Published online 22 May 2008
Subject Categories: molecular biology of disease
Keywords: kidney cyst; primary cilium; PTEN; VHL

Introduction

Inheritance of a mutant allele of the von Hippel–Lindau tumour suppressor gene (*VHL*) predisposes affected individuals to develop diverse tumours, including renal cysts and clear cell renal cell carcinoma (ccRCC) (Lonser *et al*, 2003; Kim and Kaelin, 2004). *VHL* mutation, deletion or silencing also frequently occurs in sporadic forms of these tumours. As a subset of cysts in VHL patients contain micro-foci of ccRCC, kidney cysts may, at least for a subgroup of cases, represent precursor lesions for ccRCC (Solomon and Schwartz, 1988; Choyke *et al*, 1992). However, small regions of ccRCC can also be found that are not associated with cysts, implying that a cystic precursor is not a prerequisite for ccRCC formation in all cases.

pVHL, the product of the *VHL* locus, has been ascribed several distinct biochemical activities and implicated in the regulation of diverse cellular processes, almost all of which could be envisaged to contribute to its function as a tumour suppressor protein. These include targeting the hypoxia-inducible factor α (HIFα) transcription factors for oxygen-dependent degradation, regulation of microtubule stability, maintenance of the primary cilium, activation of p53, control of neural apoptosis, suppression of epithelial to mesenchymal transition, secretion of extracellular matrix components (reviewed in Frew and Krek, 2007) and regulation of NFκB activity (Yang *et al*, 2007).

Although pVHL clearly regulates multiple signalling pathways, loss of pVHL function alone appears to be insufficient for tumour initiation in the kidney. Kidneys of patients with familial VHL disease typically contain many thousands of sites at which pVHL function has been lost; however, the vast majority of these lesions are single cells (Mandriota *et al*, 2002). Cysts occur relatively infrequently and carcinoma less frequently still. $Vhlh^{+/-}$ mice (Haase *et al*, 2001) or mice in which *Vhlh* was mosaically deleted under the control of the ubiquitously expressed β-actin promoter (Ma *et al*, 2003) are not predisposed to develop cysts or ccRCC. Cre-mediated deletion of *Vhlh* in the liver and in renal proximal tubule epithelial cells under the control of the *PEPCK-Cre* transgene likewise failed to give rise to a highly penetrant cystic phenotype, although approximately 20% of mice older than 1 year developed kidney cysts (Rankin *et al*, 2006). These observations suggest that multiple genetic mutations are required to cause progression from *VHL* mutant single-celled lesions to cysts and/or carcinomas in kidneys in VHL disease. These genetic alterations may either enhance the operation of signalling pathways already engaged upon pVHL inactivation and/or disrupt additional pathways that function cooperatively to promote tumour cell evolution.

Mutations that impair the structure or function of the primary cilium, a microtubule-based cellular sensory organelle, lead to kidney cysts in humans and in mice (reviewed in Nauli and Zhou, 2004; Pan *et al*, 2005). In cell culture systems, we have recently identified a cooperative function of pVHL and phosphatidylinositol-3-kinase (PI3K) and glycogen synthase kinase 3β (GSK3β) signalling in the maintenance of the primary cilium (Thoma *et al*, 2007a). Although pVHL-deficient primary cells form cilia normally under conditions of serum starvation, loss of pVHL sensitises cells to lose their primary cilia in response to inhibition of GSK3β or to serum-induced activation of phosphatidylinositol-3-kinase (PI3K) signalling (Thoma *et al*, 2007a). As PI3K-mediated activation of protein kinases including AKT (Cross *et al*, 1995) and p70S6K (Zhang *et al*, 2006) leads to the phosphorylation and inactivation of GSK3β, it is noteworthy that GSK3β was subjected to inhibitory phosphorylation in *VHL* mutant

*Corresponding author. Institute of Cell Biology, ETH Zurich, ETH-Honggerberg, 8093 Zurich, Switzerland. Tel.: +41 44 633 3447; Fax: +41 01 633 1357; E-mail: wilhelm.krek@cell.biol.ethz.ch

Received: 6 February 2008; accepted: 23 April 2008; published online: 22 May 2008

cysts in VHL patients, but was not phosphorylated in lesions containing only a few *VHL* mutant cells (Thoma *et al*, 2007a). On the basis of these results, it is tempting to speculate that *in vivo* cyst formation in VHL disease requires secondary mutations in *VHL* mutant cells that lead to the activation of the PI3K pathway, at least one consequence of which would be the inactivation of GSK3β and the resulting failure to maintain the primary cilium.

Aberrant activation of the PI3K signalling pathway through loss of negative regulators, such as the PTEN tumour suppressor protein, or oncogenic activation of positive mediators, such as PI3K and AKT kinases, are frequent events in many human tumours. Importantly, loss of heterozygosity of *PTEN* (Velickovic *et al*, 2002) and reduction of expression of PTEN protein (Shin Lee *et al*, 2003), as well as activation of AKT (Horiguchi *et al*, 2003; Pantuck *et al*, 2007), correlate with poor patient outcome in sporadic cases of ccRCC. These observations suggest that there may be a cooperative effect of loss of pVHL and PTEN functions in kidney tumorigenesis.

In this study, we demonstrate that cysts in human VHL patients exhibit hyperactivation of several components of the PI3K and mTOR signalling pathways. Indeed, deletion of *Vhlh* and *Pten* in distal tubules of the kidney in mice causes the formation of cysts at young age and with high penetrance. Importantly, these cysts are characterised by a reduced frequency of primary cilia. We propose that hyperactivation of the PI3K pathway, for example through loss of PTEN, represents one cooperating mechanism that leads to disease progression in familial and sporadic VHL-associated kidney disease.

Results

Hyperactivation of the PI3K signalling pathway in VHL mutant cysts

To investigate whether hyperactivation of the PI3K signalling pathway occurs in cysts in VHL disease, we immunohistochemically stained a set of serial sections derived from four previously described kidney biopsies from three VHL patients (Thoma *et al*, 2007a) using antibodies against CA9, phospho-Ser473 AKT, phospho-Ser9 GSK3β, phospho-Thr389 p70S6K and phospho-Ser240/244 S6 ribosomal protein to investigate the activation state of downstream components of the PI3K signalling pathway. Histologically normal regions of kidneys that contained only isolated *VHL* mutant cells, as identified by immunohistochemical staining for the HIFα target gene CA9 (Figure 1A), contained only occasional cells that stained for the above-mentioned markers. In contrast, 33 of 33 *VHL* mutant cystic lesions, which were mostly lined with a single-layered epithelium (simple cysts; Figure 1B, E, H, K and N), but in some cases contained micro-foci of ccRCC (atypical cysts; Figure 1C, F, I, L and O), all displayed staining for the tested antibodies. No staining was observed when primary antibodies were omitted and primary antibodies against other proteins (including phospho-PKCζ and active-β-catenin) did not reveal specific upregulation in cystic cells (data not shown), demonstrating the specificity of the depicted staining.

Although we cannot formally exclude that isolated *VHL* mutant cells may display activation of the PI3K pathway (due to a lack of sensitivity of the phospho-specific antibodies in immunofluorescence staining that prevented co-staining experiments), we quantified the staining frequency of three antibodies that gave the strongest signals in immunohistochemistry. In regions of normal kidney tissue from these biopsies, the anti-CA9 antibody stained 303 individual cells, whereas the anti-phospho-Ser240/244 S6 ribosomal protein antibody stained only 86 individual cells and the anti-phospho-Ser9 GSK3β antibody stained only 46 individual cells. These cells were morphologically identical to surrounding cells. As many fewer cells display markers of activation of PI3K signalling than loss of pVHL function, these results suggest that *VHL* mutant cells do not automatically display activation of PI3K signalling and imply that hyperactivation of the PI3K pathway may potentially be an early event and contributing factor in the formation of cystic and tumorigenic lesions in VHL patients.

Combined Vhlh and Pten mutation causes kidney cysts

Although the precise cell type of origin of ccRCC remains controversial, *VHL* mutant multicellular lesions arise almost exclusively in the distal tubules in human VHL patients (Mandriota *et al*, 2002). To investigate the physiological effect of *Vhlh* deletion in distal tubule epithelial cells of the kidney, we crossed mice with a loxP-flanked *Vhlh* allele ($Vhlh^{fl/fl}$) (Haase *et al*, 2001) to *Ksp1.3-Cre* transgenic mice (Shao *et al*, 2002). This transgene induces Cre-mediated recombination widely throughout the renal epithelium, including in distal tubules, ascending and descending loops of Henle and collecting ducts, but rarely in proximal tubules.

Deletion of *Vhlh* in kidneys of *Ksp1.3-Cre;* $Vhlh^{fl/fl}$ mice (hereafter referred to as $Vhlh^{\Delta/\Delta}$) was confirmed by PCR-mediated detection of the recombined *Vhlh* allele (Figure 2A) (Haase *et al*, 2001). Cohorts of $Vhlh^{\Delta/\Delta}$ mice were analysed at 2–3 ($n=8$), 3–5 ($n=6$) and 11–13 months ($n=9$) of age. $Vhlh^{\Delta/\Delta}$ kidneys were of normal external appearance (not shown) and parenchymal mass (Figure 2C) but displayed fully penetrant hydronephrosis, characterised by an expansion of the renal pelvis (Supplementary Figure 1B). Blockage of urinary flow induces hydronephrosis in various mammals, including mice (Ophascharoensuk *et al*, 1999). However, $Vhlh^{\Delta/\Delta}$ mice did not display histological abnormalities in the urothelium of the renal pelvis (Supplementary Figure 1F) or the urether (data not shown), tissues in which Cre activity is also present, suggesting that blockage of urinary flow does not account for the hydronephrosis. Importantly, at all ages examined, $Vhlh^{\Delta/\Delta}$ mice did not display histological abnormalities in the structure of the tubules in the kidney cortex (Figure 2E) or medulla (data not shown). These findings are consistent with the previously published mouse and human data that loss of pVHL alone does not automatically lead to cysts or ccRCC (Mandriota *et al*, 2002; Rankin *et al*, 2006).

To genetically test the effect of constitutive activation of PI3K signalling in the kidney, we utilised mice with a loxP-flanked *Pten* allele ($Pten^{fl/fl}$) (Lesche *et al*, 2002) to generate *Ksp1.3-Cre;* $Pten^{fl/fl}$ (hereafter referred to as $Pten^{\Delta/\Delta}$) and *Ksp1.3-Cre;* $Vhlh^{fl/fl}$; $Pten^{fl/fl}$ (hereafter referred to as $Vhlh^{\Delta/\Delta}Pten^{\Delta/\Delta}$) mice, in which the *Pten* tumour suppressor, which normally opposes the activity of PI3K, was deleted in a wild-type or *Vhlh* mutant background, respectively.

Deletion of *Pten* in kidneys of $Pten^{\Delta/\Delta}$ mice was confirmed by PCR-mediated detection of the recombined *Pten* allele (Figure 2A) (Lesche *et al*, 2002). Cohorts of $Pten^{\Delta/\Delta}$ mice were analysed at 2–3 ($n=3$), 3–5 ($n=5$) and 11–13 months ($n=6$) of age. Kidneys of $Pten^{\Delta/\Delta}$ mice were not significantly

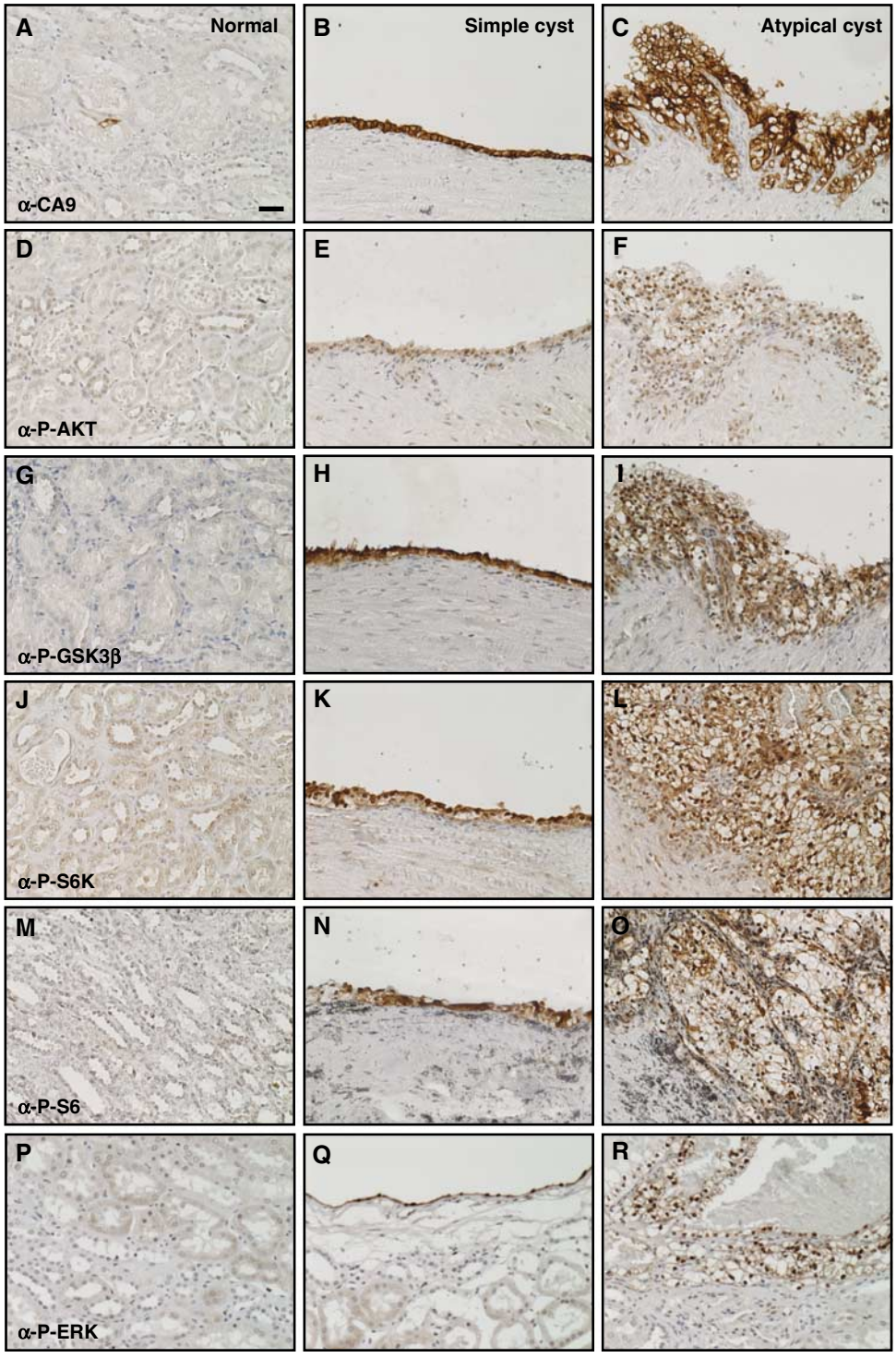

Figure 1 PI3K pathway and ERK signalling are upregulated in kidney cysts in VHL patients. Immunohistochemical analysis of sections from a single VHL patient showing (**A**, **D**, **G**, **J**, **M**, **P**) histologically normal kidney tissue, (**B**, **E**, **H**, **K**, **N**, **Q**) a cyst lined by a single epithelial layer (simple cyst) and (**C**, **F**, **I**, **L**, **O**, **R**) a cyst lined with multilayered and disorganised epithelial cells (atypical cyst). Sections were stained with antibodies against (A–C) carbonic anhydrase 9, (D–F) phopho-Ser473 AKT, (G–I) phospho-Ser9 GSK3β, (J–L) phospho-Thr389 p70S6K, (M–O) phospho-Ser240/244 S6 ribosomal protein and (P–R) phospho-Thr202/Tyr204 ERK1/2. All panels are the same magnification, bar = 20 μm. Images shown in (B, E, H, K, N, Q) and in (C, F, I, L, O, R) are derived from an equivalent region in adjacent (but not serial) sections and are representative of staining seen in multiple cysts in each of four separate kidney biopsies.

different to controls in mass (Figure 2C), and tubules within the cortex and medulla appeared histologically normal at all ages examined (Figure 2F and Supplementary Figure 1C). The urothelium of the renal pelvis (Supplementary Figure 1G), urether and bladder (not shown) displayed a similar phenotype to that previously published for the deletion of *Pten* in the bladder and urether (Tsuruta *et al*, 2006; Yoo *et al*, 2006), namely hyperproliferation and enlarged epithelial cells. Unlike in $Vhlh^{\Delta/\Delta}$ mice, kidneys from $Pten^{\Delta/\Delta}$ mice did not display hydronephrosis (Supplementary Figure 1C).

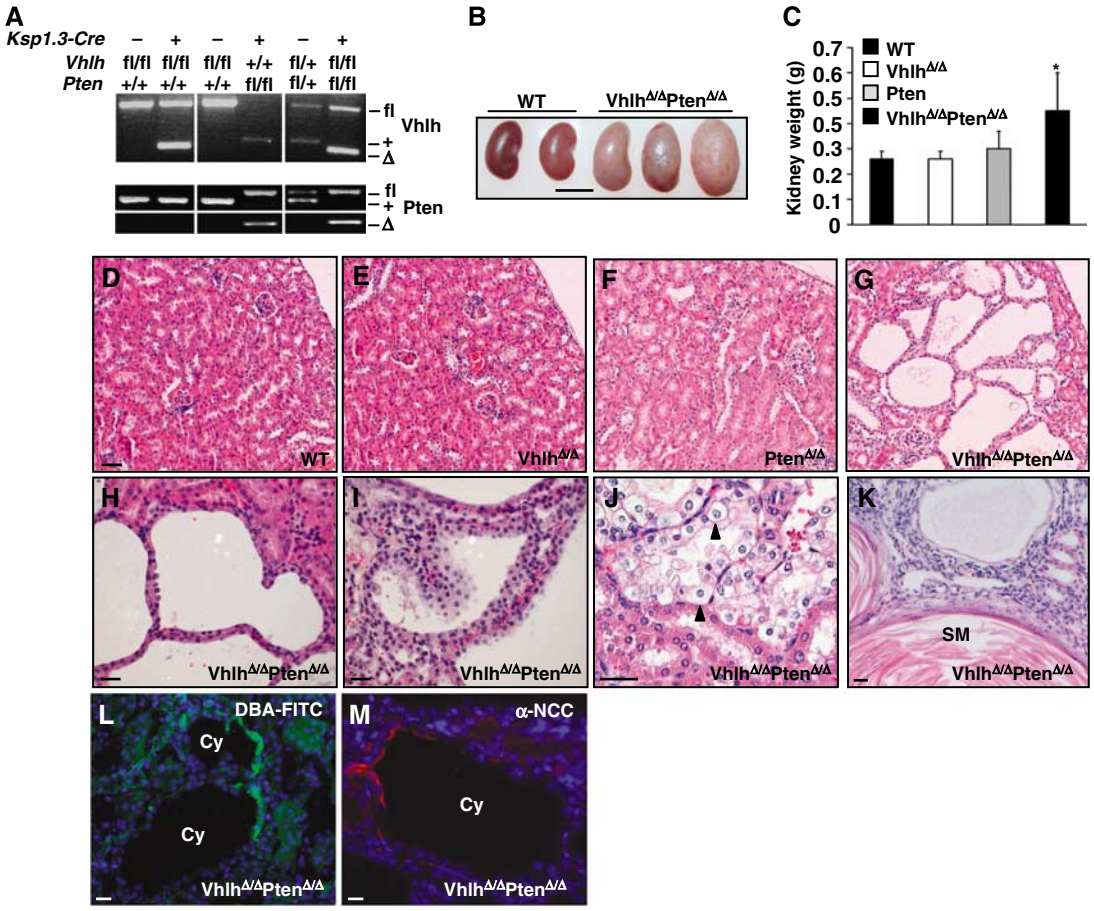

Figure 2 Analysis of $Vhlh^{\Delta/\Delta}$, $Pten^{\Delta/\Delta}$ and $Vhlh^{\Delta/\Delta}Pten^{\Delta/\Delta}$ mice. (**A**) PCR analysis of recombination at the *Vhlh* and *Pten* loci in mice with combinations of the *Ksp1.3-Cre* transgene and *Vhlh* and *Pten* floxed and wild-type alleles. The positions of the bands representing the *Vhlh* and *Pten* floxed (fl), wild type (+) and recombined (Δ) alleles are indicated. (**B**) Comparison of the size and external morphology of WT and $Vhlh^{\Delta/\Delta}Pten^{\Delta/\Delta}$ kidneys (bar = 1 cm). (**C**) Mass of kidneys from WT, $Vhlh^{\Delta/\Delta}$, $Pten^{\Delta/\Delta}$ and $Vhlh^{\Delta/\Delta}Pten^{\Delta/\Delta}$ mice ($n \geqslant 9$, aged 8–21 weeks). $^*P < 0.01$, Student's *t*-test. (**D**–**G**) Histological appearance of renal cortex from littermate 8-week-old WT, $Vhlh^{\Delta/\Delta}$, $Pten^{\Delta/\Delta}$ and $Vhlh^{\Delta/\Delta}Pten^{\Delta/\Delta}$ mice (bar = 100 μm). Examples of (**H**) simple and (**I**) atypical cysts, (**J**) clear cell morphology (arrowheads) and (**K**) a region of squamous metaplasia (SM) characterised by keratinocyte-like cells surrounding a core of keratin (pink staining), in $Vhlh^{\Delta/\Delta}Pten^{\Delta/\Delta}$ renal cortex. Immunofluorescence staining for (**L**) the collecting duct marker FITC-tagged *Dolichos biflorus* agglutinin and (**M**) the distal tubule marker NaCl cotransporter in cysts in $Vhlh^{\Delta/\Delta}Pten^{\Delta/\Delta}$ renal cortex. Bars in (H–M) = 10 μm.

Combined deletion of *Vhlh* and *Pten* in $Vhlh^{\Delta/\Delta}Pten^{\Delta/\Delta}$ mice (Figure 2A) resulted in a similar hydronephrosis phenotype (Supplementary Figure 1D) to that seen in $Vhlh^{\Delta/\Delta}$ kidneys and a more pronounced hyperproliferation of the urothelium (Supplementary Figure 1H) than that of $Pten^{\Delta/\Delta}$ mice. Kidneys from mice with combinations of homozygous and heterozygous *Vhlh* and *Pten* deletion ($Vhlh^{\Delta/\Delta}Pten^{\Delta/+}$ ($n = 8$) and $Vhlh^{\Delta/+}Pten^{\Delta/\Delta}$ ($n = 5$)) were indistinguishable from those of $Vhlh^{\Delta/\Delta}$ and $Pten^{\Delta/\Delta}$ mice, respectively. Strikingly, male and female $Vhlh^{\Delta/\Delta}Pten^{\Delta/\Delta}$ mice had enlarged and heavier kidneys (Figure 2B and C) due to the formation of multiple epithelial tubule cysts in the cortex and medulla (Figure 2G and Supplementary Figure 1D). Cysts were present in kidneys from 14 of 14 mice and were detected as early as 6–8 weeks of age. The majority of cysts were lined by a single layer of epithelial cells (simple cysts) (Figure 2H), whereas approximately 8% of cysts (21 of 269 cysts from three mice) were lined by multilayered epithelial cells with occasional papillary projections (atypical cysts) (Figure 2I). Cells lining all cysts displayed clear cell morphology (Figure 2J), mimicking the histological changes seen upon pVHL loss in human kidneys (Mandriota *et al*, 2002). Three of 14 kidneys displayed isolated regions of benign squamous metaplasia within the cortex (Figure 2K). $Vhlh^{\Delta/\Delta}Pten^{\Delta/\Delta}$ mice were killed within 3–6 months of birth to avoid renal failure. No overt tumours or even small areas of adenoma or carcinoma were observed within this time frame in the kidney. Staining with *Dolichos biflorus* agglutinin (Figure 2L) and with an antibody against the Na-Cl co-transporter (Figure 2M) demonstrated that cysts arose in collecting ducts and distal tubules, respectively. Interestingly, cysts often contained only a few cells that stained positively for these markers (perhaps reflecting cells in which Cre-mediated recombination had not taken place) and in many cysts there was no staining at all, consistent with a possible de-differentiation of these cells, as postulated for the cysts that develop in *PEPCK-Cre*; *Vhlh* mutant mice (Rankin *et al*, 2006). A similar phenomenon was seen in human VHL patients where *VHL* mutant cells within a histologically normal distal kidney tubule lost expression of Tamm-Horsfall protein, a distal tubule marker (Mandriota *et al*, 2002). Consistent with the expression pattern of the Cre transgene, we observed no cysts that stained positively for the proximal tubule marker *Lotus tetragonolobus* lectin.

Immunohistochemical staining for the proliferation marker Ki-67, which is expressed by proliferating, but not by resting cells, demonstrated that although epithelial cell proliferation was not significantly increased by deletion of *Vhlh* (Figure 3B) or *Pten* (Figure 3C) alone, cysts in $Vhlh^{\Delta/\Delta}Pten^{\Delta/\Delta}$ mice displayed an approximately 3- to 6-fold increase in staining for Ki-67 (Figure 3D and E). In summary, simple and atypical cystic proliferative lesions that resemble the lesions seen in distal tubules in VHL patients arise in the kidneys of $Vhlh^{\Delta/\Delta}Pten^{\Delta/\Delta}$ mice.

HIFα activation is not sufficient for cyst formation

As activation of the PI3K pathway has been shown to enhance the translation of HIFα, and as pVHL regulates the proteolytic degradation of HIFα, we investigated the activation status of the HIFα proteins in *Vhlh* and *Pten* mutant kidneys. Immunohistochemical staining revealed that mutation of *Vhlh* but not of *Pten* leads to strong, primarily nuclear accumulation of HIF1α (Figure 4B and C) and HIF2α (Figure 4F and G) in epithelial cells in tubule types that are known to express Cre. Epithelial cells lining cysts in $Vhlh^{\Delta/\Delta}Pten^{\Delta/\Delta}$ kidneys also exhibited strong nuclear accumulation of HIF1α (Figure 4D) and HIF2α (Figure 4H), demonstrating that cystic cells had arisen from cells in which Cre-mediated recombination had occurred. High levels of the HIFα target protein LDH-A were also observed in tubules of kidneys from $Vhlh^{\Delta/\Delta}$ (Figure 4J) and $Vhlh^{\Delta/\Delta}Pten^{\Delta/\Delta}$ (Figure 4L) mice, demonstrating that HIFα was transcriptionally active.

Western blotting of whole kidney lysates for phospho-Ser473 AKT confirmed activation of the PI3K signalling pathway in $Vhlh^{\Delta/\Delta}Pten^{\Delta/\Delta}$ kidneys (Figure 4U). To quantitatively assess whether loss of HIFα degradation due to loss of pVHL combined with potentially enhanced HIFα translation due to loss of PTEN might lead to an overall increase in HIFα activity, we analysed the mRNA and protein abundance of various known HIFα target genes in mutant kidneys. Western blotting for the HIFα-inducible proteins GLUT-1, LDH-A and PDK-1 (Figure 4U) and real-time PCR analysis of the HIFα target genes *Glut-1*, *Ca9*, *Pgk-1*, *Vegf-a*, *BNip3* and *Redd1* (Figure 4V) revealed increased HIFα target gene expression in $Vhlh^{\Delta/\Delta}$ and $Vhlh^{\Delta/\Delta}Pten^{\Delta/\Delta}$ kidneys. Although there was a trend towards higher HIFα target gene expression in kidneys

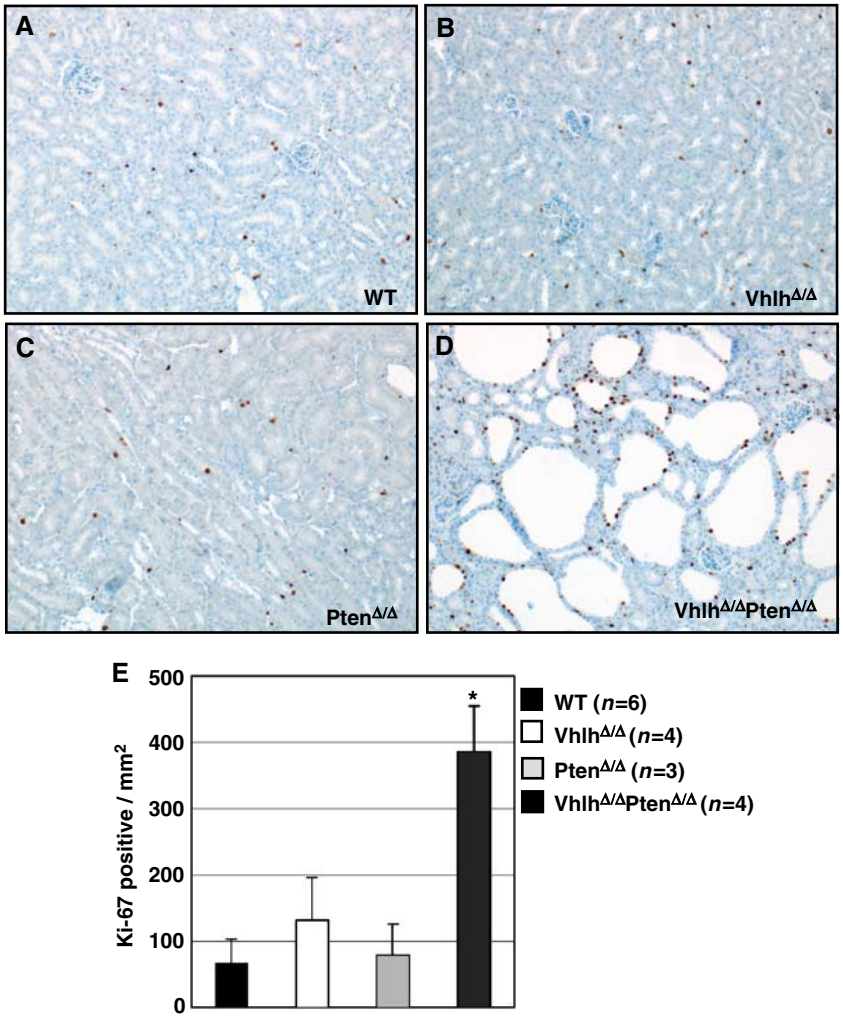

Figure 3 Increased proliferation in kidneys of $Vhlh^{\Delta/\Delta}Pten^{\Delta/\Delta}$ mice. (**A–D**) Immunohistochemical analysis of kidney cortex from WT (A), $Vhlh^{\Delta/\Delta}$ (B), $Pten^{\Delta/\Delta}$ (C) and $Vhlh^{\Delta/\Delta}Pten^{\Delta/\Delta}$ (D) mice using an antibody against the proliferation marker Ki-67. (**E**) Quantification of the number of epithelial cells per mm^2 of the kidney cortex that express Ki-67. One field per kidney section (between three and six mice of each genotype, aged between 8–12 weeks) was counted and the data represent mean ± standard deviation. *Statistically significant ($P<0.001$, Student's *t*-test) difference between $Vhlh^{\Delta/\Delta}Pten^{\Delta/\Delta}$ and all other genotypes.

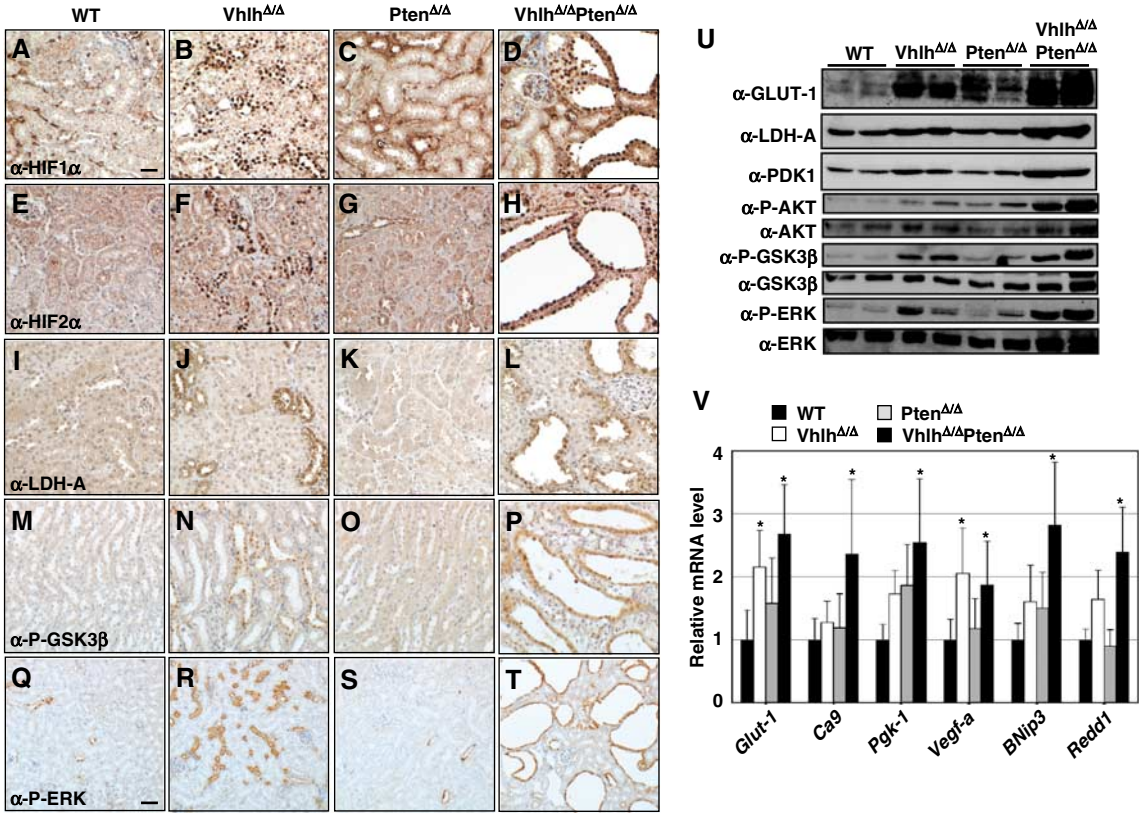

Figure 4 Analysis of HIFα activation and PI3K signalling in kidneys of WT, Vhlh$^{\Delta/\Delta}$, Pten$^{\Delta/\Delta}$ and Vhlh$^{\Delta/\Delta}$Pten$^{\Delta/\Delta}$ mice. Immunohistochemical analysis of kidney sections from WT (**A**, **E**, **I**, **M**, **Q**), Vhlh$^{\Delta/\Delta}$ (**B**, **F**, **J**, **N**, **R**), Pten$^{\Delta/\Delta}$ (**C**, **G**, **K**, **O**, **S**) and Vhlh$^{\Delta/\Delta}$Pten$^{\Delta/\Delta}$ (**D**, **H**, **L**, **P**, **T**) mice. Sections were stained with antibodies against (A–D) HIF1α, (E–H) HIF2α, (I–L) LDH-A, (M–P) phospho-Ser9 GSK3β and (Q–T) phospho-Thr202/Tyr204 ERK1/2. (A–P) are the same magnification, bar = 20 μm, (Q–T) are the same magnification, bar = 40 μm. (U) Whole kidney protein lysates from two mice of each indicated genotype were analysed by western blotting using antibodies against GLUT-1, LDH-A, PDK1, phospho-Ser473 AKT (P-AKT), AKT, phospho-Ser9 GSK3β (P-GSK3β), GSK3β, phospho-Thr202/Tyr204 ERK1/2 (P-ERK) and anti-ERK1/2 (ERK). (V) cDNA prepared from whole kidney RNA extracts was analysed by real-time quantitative PCR using specific primers for *Glut-1*, *Ca9*, *Pgk-1*, *Vegf-a*, *BNip3* and *Redd1*. Fold expression changes were normalised against the expression level of the 18S ribosomal RNA. Data represent mean ± standard deviation of four or five mice of each genotype, each sample analysed in triplicate. *Statistically significant ($P<0.05$, ANOVA followed by Dunnett's two-tailed test) differences in gene expression in comparison to wild type. There were no statistically significant differences between Vhlh$^{\Delta/\Delta}$ and Vhlh$^{\Delta/\Delta}$Pten$^{\Delta/\Delta}$ mice.

of Vhlh$^{\Delta/\Delta}$Pten$^{\Delta/\Delta}$ mice than in kidneys of Vhlh$^{\Delta/\Delta}$ or Pten$^{\Delta/\Delta}$ mice, this trend is most likely attributable to the greater proportion of *Vhlh*-negative cells in whole kidney RNA extracts from Vhlh$^{\Delta/\Delta}$Pten$^{\Delta/\Delta}$ kidneys due to the presence of an expanded population of *Vhlh*-negative cells in cysts. Although we cannot exclude that *Pten* mutation may contribute to cyst formation by selectively altering the pattern or magnitude of expression of a subset of HIFα target genes, collectively these findings demonstrate that activation of HIF1α and HIF2α following *Vhlh* mutation alone are not sufficient to cause kidney pathology and suggest that the cooperative suppression of cyst formation by *Vhlh* and *Pten* likely involves mechanisms that are independent of, or additional to, HIFα.

Reduced frequency of primary cilia in Vhlh$^{\Delta/\Delta}$Pten$^{\Delta/\Delta}$ cysts

Defects in function or structure of the primary cilium cause kidney cyst formation (reviewed in Nauli and Zhou, 2004; Pan *et al*, 2005) and cystic epithelial cells in VHL patients frequently lack a primary cilium (Thoma *et al*, 2007a). As loss of pVHL function sensitises cells to lose their primary cilia in response to PI3K-dependent signalling (Thoma *et al*, 2007a), we analysed cysts in kidneys of Vhlh$^{\Delta/\Delta}$Pten$^{\Delta/\Delta}$ mice for the presence of primary cilia by immunofluorescence staining for acetylated tubulin. In contrast to distal tubules in wild-type (Figure 5A), Vhlh$^{\Delta/\Delta}$ (Figure 5B) and Pten$^{\Delta/\Delta}$ (Figure 5C) kidneys, in which 80–90% of epithelial cells were ciliated (Figure 5E), distal tubule cysts in Vhlh$^{\Delta/\Delta}$Pten$^{\Delta/\Delta}$ kidneys displayed only approximately 30% ciliated cells (Figure 5E; non-ciliated cells indicated by arrowheads in Figure 5D). In comparison, non-cystic distal tubules in Vhlh$^{\Delta/\Delta}$Pten$^{\Delta/\Delta}$ kidneys contained normal frequencies of ciliated epithelial cells (Figure 5E), further emphasising the connection between loss of primary cilia and cyst formation. Combined with our previous findings (Thoma *et al*, 2007a), these data suggest that loss of *Vhlh* and *Pten* leads to failure of kidney epithelial cells to maintain their primary cilia, resulting in uncontrolled proliferation and cyst formation.

Multiple signalling pathways control cilia in pVHL-deficient cells

To investigate whether there is a cell-autonomous requirement for pVHL and PTEN in cilia formation or cilia maintenance, we performed cilia assays using cultured cells. h-TERT-immortalised human retinal pigment epithelium

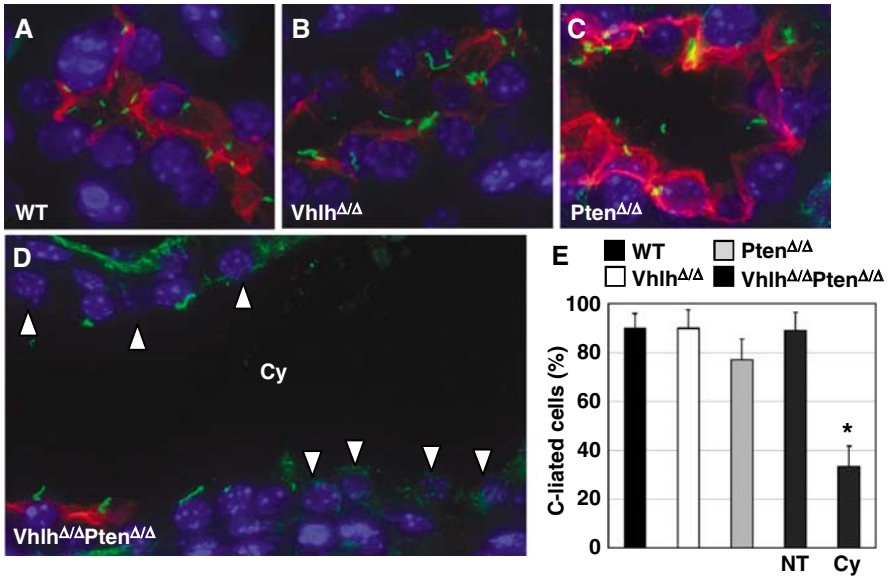

Figure 5 Analysis of primary cilia in distal tubules of WT, Vhlh$^{\Delta/\Delta}$, Pten$^{\Delta/\Delta}$ and Vhlh$^{\Delta/\Delta}$Pten$^{\Delta/\Delta}$ mice. Kidney sections from (**A**) WT, (**B**) Vhlh$^{\Delta/\Delta}$, (**C**) Pten$^{\Delta/\Delta}$ and (**D**) Vhlh$^{\Delta/\Delta}$Pten$^{\Delta/\Delta}$ mice were stained with antibodies against NaCl cotransporter (red) and acetylated tubulin (green) and with DAPI to label distal tubules, cilia and nuclei, respectively. Arrowheads in (D) depict cells that lack primary cilia. (**E**) Quantitation of cilia frequency in distal tubule epithelial cells in WT, Vhlh$^{\Delta/\Delta}$ and Pten$^{\Delta/\Delta}$ kidneys and in normal (NT) and cystic (Cy) distal tubules in Vhlh$^{\Delta/\Delta}$Pten$^{\Delta/\Delta}$ kidneys. Data represent mean ± standard deviation of analysis of between 6 and 16 distal tubules (representing 100–730 cells) of each genotype. $^{*}P = 0.002$, Student's *t*-test.

(RPE-1) were chosen for analysis as they represent a non-transformed human epithelial cell line that readily forms primary cilia and can be easily manipulated genetically. Consistent with our previous findings in other cell systems (Thoma *et al*, 2007a), knockdown of *VHL* sensitised RPE-1 cells to lose their already established primary cilia in response to serum re-addition for 4 h (Figure 6A). Knockdown of *AKT1* rescued the effect of serum on *VHL* knockdown cells (Figure 6A), demonstrating genetically that AKT1 activity contributes to cilia loss and supporting earlier data that suggested the requirement of a wortmannin-sensitive signalling pathway for serum-induced cilia loss in *VHL*-negative cells (Thoma *et al*, 2007a). However, although knockdown of *PTEN* led to elevated AKT activity (Figure 6C), *VHL/PTEN* double knockdown cells were still able to form cilia normally following serum starvation and lost their cilia equivalently to *VHL* knockdown cells following serum re-stimulation (Figure 6A). These findings suggest that although AKT activity is necessary, constitutive AKT activity alone is not sufficient to cooperate with loss of pVHL to cause cilia loss. Supporting this conclusion, *Vhlh* and/or *Pten* were deleted from primary mouse embryo fibroblasts (MEFs) derived from wild-type, *Vhlh*$^{fl/fl}$, *Pten*$^{fl/fl}$ or *Vhlh*$^{fl/fl}$*Pten*$^{fl/fl}$ mice by infection with a non-genotoxic Cre-expressing lentivirus and the cells were subjected to cilia formation assays. There were no differences among the genotypes in the frequency of ciliated cells following serum starvation for 12, 24, 48 or 72 h (Figure 6D), despite the maintenance of AKT activity in *Pten* and *Vhlh/Pten* mutant cells even after 72 h of growth in the absence of serum (Figure 6E). *Vhlh/Pten* double mutant cells lost their primary cilia in response to serum restimulation equivalently to *Vhlh* single mutant cells (data not shown).

Although AKT activation is a necessary but not sufficient component of a serum-induced signalling pathway that causes loss of cilia in pVHL-deficient cells, we reasoned that additional signalling pathways might be required for this response and therefore attempted to pharmacologically define the molecular requirements for cilia loss. Immortalised MEFs expressing control non-silencing or short hairpin RNA interference against *Vhlh* (Thoma *et al*, 2007a) were serum starved for 3 days to induce cilia formation and pretreated with inhibitors against PI3K (LY294,002), mTOR (RAD001), MEK (U0126), ERK (ERK inhibitor II), PKCζ (myristoylated PKCζ pseudosubstrate) or JNK (JML), prior to serum re-stimulation in the presence of inhibitor for 4 h. The PKCζ and JNK inhibitors alone altered microtubule and cilia structures and were therefore not useful in this setting. Western blotting confirmed the specific effects of the remaining inhibitors upon their respective signalling pathways (Figure 7B). Consistent with our previous results (Thoma *et al*, 2007a), inhibition of PI3K signalling by LY294,002 blocked cilia loss caused by serum (Figure 7A). This response is independent of mTOR activation as RAD001 failed to block cilia loss in *Vhlh*-deficient cells (Figure 7A). Interestingly, both the MEK and ERK inhibitors also potently blocked serum-induced cilia loss (Figure 7A), implicating this signalling cascade in controlling cilia loss in pVHL-deficient cells. Thus, serum-induced activation of AKT as well as of MEK-ERK appears to be required for the loss of cilia when pVHL is not present. As deletion of *Vhlh* and *Pten* causes AKT activation but not ERK activation in serum-starved cultured cells (Figure 6E), this finding may explain why *Vhlh/Pten* mutant cells in culture do not display defects in cilia formation in response to serum starvation.

Cystic cells display activating phosphorylation of AKT and ERK and inhibitory phosphorylation of GSK3β

Given the requirement for both AKT and ERK signalling in causing cilia loss in pVHL-deficient cells in culture, we

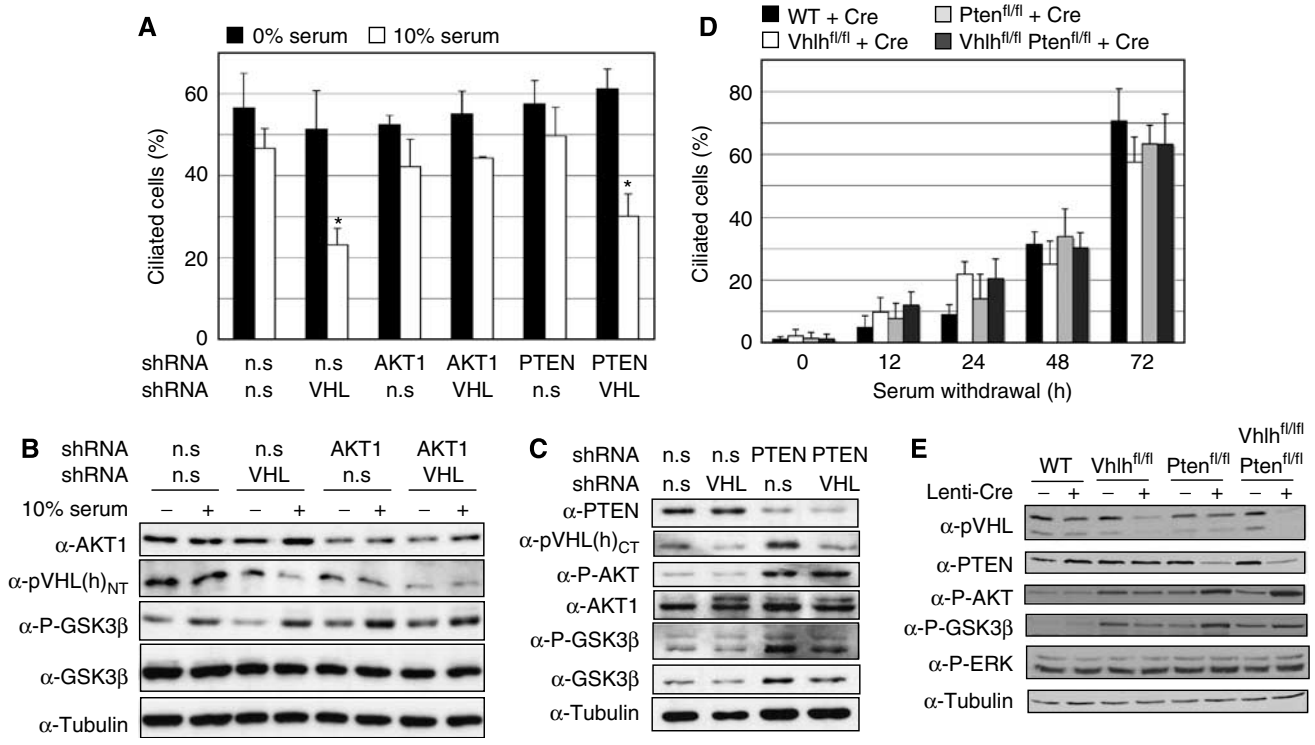

Figure 6 Loss of PTEN does not cause cilia loss in pVHL-deficient cells. (**A**) Quantitation of frequency of ciliated RPE-1 cells following short hairpin-mediated gene knockdown using vectors expressing non-silencing (n.s) or combinations of *VHL*, *AKT1* or *PTEN* hairpins. Following 3 days of serum starvation, cells were re-stimulated for 4 h with 0 or 10% serum. Data represent mean ± standard deviation of two or three independent experiments, each assayed in triplicate assays. $^*P<0.01$, Student's *t*-test. (**B**) Western analysis of RPE-1 cells after control knockdown (n.s) or knockdown of *VHL* and/or *AKT1*. Blots were probed with antibodies against AKT1, pVHL, phospho-Ser9 GSK3β (P-GSK3β), GSK3β and α-tubulin. (**C**) Western analysis of RPE-1 cells after control knockdown (n.s) or knockdown of *VHL* and/or *PTEN*. Blots were probed with antibodies against PTEN, pVHL, phospho-Ser473 AKT (P-AKT), AKT1, phospho-Ser9 GSK3β (P-GSK3β), GSK3β and α-tubulin. (**D**) Quantitation of frequency of ciliated primary MEFs derived from wild-type, $Vhlh^{fl/fl}$, $Pten^{fl/fl}$ and $Vhlh^{fl/fl}Pten^{fl/fl}$ embryos following infection with Lenti-Cre. Subconfluent cells were subjected to serum starvation for the indicated times. Data represent mean ± standard deviation of triplicate assays and are representative of data seen in one (12, 24 and 48 h time points) or three (72 h time point) independent experiments. (**E**) Western analysis of cells from (D) that were grown for 3 days in the absence of serum prior to harvesting. Blots were probed with antibodies against PTEN, pVHL, phospho-Ser473 AKT (P-AKT), phospho-Ser9 GSK3β (P-GSK3β), GSK3β, α-tubulin and phospho-Thr202/Tyr204 ERK1/2 (P-ERK).

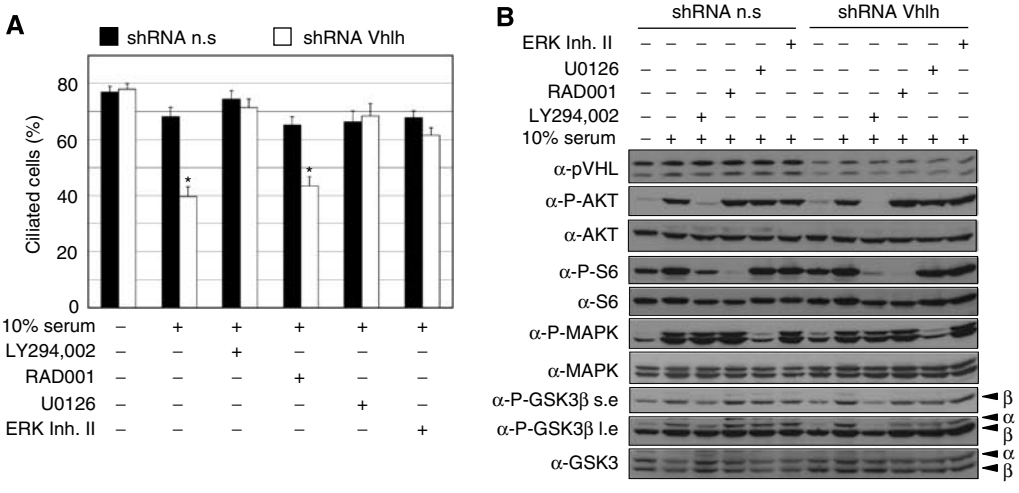

Figure 7 Multiple pathways control cilia loss in pVHL-deficient cells. (**A**) Quantitation of frequency of ciliated immortalised MEFs following short hairpin-mediated gene knockdown using vectors expressing non-silencing (n.s) or *Vhlh* knockdown hairpins. Cells were starved of serum for 3 days, treated for 70 min with indicated inhibitors prior to stimulation with 0 or 10% serum for 4 hours in the presence of the inhibitor. Data represent mean ± standard deviation of three independent experiments, each assayed in triplicate. $^*P<1\times10^{-8}$, Student's *t*-test. (**B**) Western analysis of cells from (A). Blots were probed with antibodies against pVHL, phospho-Ser473 AKT (P-AKT), AKT, phospho-Ser240/244 S6 ribosomal protein (P-S6), S6 ribosomal protein (S6), phospho-Thr202/Tyr204 ERK1/2 (P-ERK), anti-ERK1/2 (ERK), phospho-Ser9 GSK3β (P-GSK3β) and GSK3. The phospho-Ser9 GSK3β antibody cross-reacts with phosphorylated GSK3α and the positions of the respective proteins are indicated by α and β.

investigated the activation status of these signalling pathways in kidney cysts *in vivo*. Kidney lysates from $Vhlh^{\Delta/\Delta}Pten^{\Delta/\Delta}$ mice display increased expression of phospho-Ser473 AKT, phospho-Thr202/Tyr204 ERK1/2 and of phospho-Ser9 GSK3β (Figure 4U), markers of activation (AKT and ERK) or inhibition (GSK3β) of these protein kinases. Immunohistochemical staining confirmed that both phospho-Thr202/Tyr204 ERK1/2 (Figure 4P) and phospho-Ser9 GSK3β (Figure 4T) are expressed within cystic cells. Interestingly, *Vhlh* deletion alone led to an increase in expression of phospho-Ser473 AKT (Figure 4U), phospho-Ser9 GSK3β (Figure 4N and U) and of phospho-Thr202/Tyr204 ERK1/2 (Figure 4R and U), possibly attributable to the HIFα-mediated upregulation of growth factors such as TGFα or PDGF that signal through these pathways. Whereas mutation of *Pten* alone caused a mild upregulation of phospho-Ser473 AKT, the combined mutation of *Vhlh* and *Pten* resulted in the enhancement of activating phosphorylation of AKT and inhibitory phosphorylation of GSK3β (Figure 4U), possibly due to the increased sensitivity of *Pten* mutant cells to dysregulated growth factor signalling following *Vhlh* mutation. In cysts from human VHL patients, which display activation of the PI3K signalling cascade, 25 of 33 cysts also stained positively for phospho-Thr202/Tyr204 ERK1/2 (Figure 1Q and R). Thus, in two different physiological settings of VHL-associated cyst formation there is activation of two distinct signalling pathways that are necessary for cilia loss in pVHL-deficient cells. We suggest that, at the minimum, the combination of loss of pVHL function and activation of PI3K and ERK signalling is required to induce loss of cilia and subsequent cyst formation *in vivo*.

Discussion

Despite intense investigations, the molecular genetics underlying renal pathology in VHL disease remains incompletely understood. Studies of kidneys from VHL patients revealed a low frequency of multicellular, cystic lesions compared with single cell lesions, implying that the early proliferative advantage conveyed by biallelic *VHL* inactivation may be relatively modest (Mandriota *et al*, 2002). Consistent with this view, conditional inactivation of *Vhlh* in the mouse liver and kidney elicits renal cysts only after long latency with low penetrance (Rankin *et al*, 2006). Moreover, although renal cysts of VHL patients display a reduced frequency of primary cilia, consistent with the role of this sensory organelle as a suppressor of uncontrolled proliferation and cyst formation, cell biological evidence suggests that pVHL is dispensable for cilia formation in primary cells and that additional pathway(s) need to be inactivated for cells to lose their primary cilia (Frew and Krek, 2007; Thoma *et al*, 2007a, b). Here, we identify the PTEN tumour suppressor as at least one potential critical suppressor of the conversion of pVHL-deficient renal tubular epithelial cells to cysts, an initial step of kidney cancer progression.

We show that *VHL* mutant cystic lesions in VHL patients display hyperactivation of the PI3K signalling pathway and that mimicking these conditions by combined mutation of *Vhlh* and *Pten* causes kidney cysts in mice. Consistent with the role of the primary cilium as a suppressor of kidney epithelial cell proliferation, and with our previous findings that PI3K signalling in pVHL-defective cells causes loss of the primary cilium (Thoma *et al*, 2007a), cysts in $Vhlh^{\Delta/\Delta}Pten^{\Delta/\Delta}$ mice displayed a reduced frequency of primary cilia and increased proliferation. Interestingly, cysts in $Vhlh^{\Delta/\Delta}Pten^{\Delta/\Delta}$ mice developed later (6–8 weeks) than cysts that develop in other mutant mice with defects in cilia structure or function (Nauli and Zhou, 2004; Pan *et al*, 2005). Notably, deletion of *Kif3a* under the control of the *Ksp1.3-Cre* transgene, the same that was used in this study, resulted in the complete absence of cilia and caused kidney cyst formation within days of birth (Lin *et al*, 2003). The later onset of cyst formation and slower disease progression in $Vhlh^{\Delta/\Delta}Pten^{\Delta/\Delta}$ mice are consistent with our model that loss of pVHL sensitises cells to lose cilia in response to external signals (Thoma *et al*, 2007a, b), rather than being absolutely required for the formation of cilia.

We have previously shown that pVHL maintains primary cilia through its microtubule-stabilising function and that acute inhibition of GSK3β in pVHL-deficient cells causes them to lose their established primary cilia (Thoma *et al*, 2007a). Now we identify other potential components of this network and show that serum-induced activation of PI3K-AKT1 and of MEK-ERK signalling are both necessary for pVHL-deficient cells to lose their cilia. Both of these signalling pathways are activated in human *VHL* mutant cysts and in cystic kidneys of $Vhlh^{\Delta/\Delta}Pten^{\Delta/\Delta}$ mice, suggesting that the combination of PI3K activation and ERK activation may cause pVHL-mutant kidney cells to lose their primary cilia, causing proliferation and cyst formation. As ERK has been shown to phosphorylate GSK3β at Thr43, priming it for subsequent inhibitory phosphorylation at Ser9 (Ding *et al*, 2005) one possible point of intersection of these pathways is at the level of inhibition of GSK3β. We attempted to test this idea by analysing the effect of ERK inhibition on the levels of phospho-Ser9 GSK3β (Figure 7B); however, changes in total levels of GSK3β phosphorylation induced by serum were too subtle to allow a conclusion to be drawn. Further elucidation of the signalling events that cooperate with pVHL deficiency would be aided by the identification of the component(s) in serum that induces cilia loss. None of the stimuli tested, including PDGF-AA, IGF-1, insulin, FGF, TGFβ1, EGF and soluble fibronectin, were able to mimic the effects of serum on cilia loss in *Vhlh*-deficient cells, suggesting that a combination of these or other factors, in conjunction with loss of pVHL function, is required to disassemble the primary cilium in cultured cells.

The primary cilium-based model of cyst formation that we propose here needs to be viewed in light of the fact that pVHL has multiple biochemical activities. Thus, it is possible that mutation of *Pten* may also influence signalling pathways or cellular responses, such as HIFα-induced responses, NF-κB signalling, cell cycle control or epithelial to mesenchymal transition, that are dysregulated as a result of *Vhlh* mutation. Such cooperative effects of *Vhlh* and *Pten* mutation could be independent of cilia but may nonetheless contribute to dysregulated cell proliferation and cyst formation. In addition, we cannot formally exclude the possibility that alterations in urinary flow due to hyperproliferation of the urothelium in the renal pelvis and urether may also, in part, contribute to the cystic phenotype in $Vhlh^{\Delta/\Delta}Pten^{\Delta/\Delta}$ mice. Partial or complete blockage of urinary flow due to experimental manipulation or congenital abnormality can lead to a variety of kidney abnormalities, including cysts, in humans and in other mammals (Peters, 2001). Arguing against the idea that

alteration in urinary flow could wholly account for the cystic phenotype in $Vhlh^{\Delta/\Delta}Pten^{\Delta/\Delta}$ mice is the fact that $Pten^{\Delta/\Delta}$ mice also show hyperproliferation of the urothelium, albeit to a lesser extent, but do not develop kidney cysts. Additionally, cystic lesions in $Vhlh^{\Delta/\Delta}Pten^{\Delta/\Delta}$ mice uniformly display accumulation of HIFα, demonstrating that Cre-mediated recombination has occurred in these cells. If cysts arose simply due to changes in pressure within the kidney it would be expected that cysts would also occur in tubules in which Cre was not active.

One question that arises from our study is why cysts in VHL patients display hyperactivation of PI3K and ERK signalling. HIFα activation following loss of pVHL function may contribute to this effect by inducing autocrine and paracrine signalling via the upregulation of growth factors such as PDGF, VEGF or TGFα that signal via these signal-transduction pathways. It is also possible that secondary mutations, for example inhibitory mutations in *PTEN* or activating mutations in growth factor receptors, *PI3K*, *AKT*, *RAS* or *RAF* family genes, may be required to further sensitise pVHL-deficient cells to hyperactivate PI3K and ERK signalling and thereby lose cilia following growth factor signalling. An important corollary of this model is that pharmacological inhibition of the PI3K and/or ERK signalling pathways may represent therapeutic strategies to prevent the loss of primary cilia in pVHL-deficient cells and thereby inhibit cyst formation and the initial steps of ccRCC formation in VHL patients.

Materials and methods

Mouse genetics

C57BL/6J *Ksp1. 3-Cre* mice (Shao *et al*, 2002) were obtained from Peter Igarashi (UT Southwestern, USA), BALB/c;129S mixed background $Vhlh^{fl/fl}$ mice (Haase *et al*, 2001) were obtained from Jackson Labs and BALB/c $Pten^{fl/fl}$ mice (Lesche *et al*, 2002) were obtained from Andreas Trumpp (ISREC, Switzerland). *Ksp1.3-Cre/+* mice were intercrossed with $Vhlh^{fl/fl}$; $Pten^{fl/fl}$ mice to generate *Ksp1.3-Cre/+*; $Vhlh^{fl/+}$; $Pten^{fl/+}$ and +/+; $Vhlh^{fl/+}$; $Pten^{fl/+}$ mice. These mice were subsequently intercrossed to provide genetic background-matched sets of parents from which *Ksp1.3-Cre/+*; $Vhlh^{fl/fl}$; $Pten^{+/+}$ ($Vhlh^{\Delta/\Delta}$), *Ksp1.3-Cre/+*; $Vhlh^{+/+}$; $Pten^{fl/fl}$ ($Pten^{\Delta/\Delta}$) and *Ksp1.3-Cre/+*, $Vhlh^{fl/fl}$; $Pten^{fl/fl}$ ($Vhlh^{\Delta/\Delta}Pten^{\Delta/\Delta}$) mice were generated. Littermate mice that lacked the *Ksp1.3-Cre* transgene (WT) were used as controls. MEFs were derived from E13.5 wild-type (C57Bl/6J background), $Vhlh^{fl/fl}$, $Pten^{fl/fl}$ and $Vhlh^{fl/fl}$; $Pten^{fl/fl}$ mice using standard techniques.

PCR

PCR-mediated detection of Cre-mediated recombination at the *Vhlh* and *Pten* loci was performed as described (Haase *et al*, 2001; Lesche *et al*, 2002).

Immunohistochemistry and immunofluorescence

Immunohistochemistry and immunofluorescence staining were performed as previously described (Thoma *et al*, 2007a) using the following antibodies: anti-HIF1α (Santa Cruz; sc-8711), anti-CXCR4 (Santa Cruz; sc-6279), anti-CA9 (Pastorekova *et al*, 1992; M75, gift of Jan Zavada), anti-phospho-Ser473 AKT (Cell Signaling Technology; no. 9277), anti-phospho-Ser9 GSK3β (Cell Signaling Technology, no. 2215), anti-phospho-Thr389 p70S6K (Santa Cruz; sc-11759), anti-phospho-Ser240/244 S6 ribosomal protein (Cell Signaling Technology; no. 2215), anti-phospho-Thr202/Tyr204 ERK1/2 (Cell Signaling Technology; no. 9101), anti-Ki-67 (DakoCytomation; clone TEC-3), anti-LDH-A (Santa Cruz; sc-27230), anti-NaCl-cotransporter (Chemicon; AB3553) and anti-acetylated tubulin (Sigma; no. T6793). Immunohistochemistry using anti-HIF1α (Novus Biologicals; NB100-105) and anti-HIF2α (Pollard *et al*, 2007; PM8) antibodies was performed using the DakoCytomation Catalyzed Signal Amplification System. Collecting ducts were labelled by incubating kidney sections with FITC-tagged *D. biflorus* agglutinin (20 μg/ml; Vector Laboratories).

Western blotting

Cultured cells were lysed in TNN buffer (25 mM Tris–HCl pH 7.2, 500 mM sodium chloride, 10% glycerol, 1% NP-40, 10 mM sodium fluoride, 1 mM Na_3VO_4, 1 mM PMSF, 1 mM dithiothreitol, 10 μg/ml aprotinin) and whole kidney protein extracts were prepared by powdering fresh frozen kidneys under liquid nitrogen followed by homogenisation in TNN buffer. Protein extracts (60 μg) were run on 8–15% polyacrylamide gels, transferred to nitrocellulose membranes and visualised by immunoblotting with the following antibodies: anti-GLUT-1 (Abcam; ab14683), anti-LDH-A (Santa Cruz; sc-27230), anti-PDK-1 (Stressgen; KAP-PK112), anti-phospho-Ser473 AKT (Cell Signaling Technology; no. 4058), anti-AKT (Santa Cruz; sc-1619), anti-AKT1 (2H10, Cell Signaling Technology; no. 2967), anti-phospho-Ser9 GSK3β (Cell Signaling Technology; no. 2215), anti-GSK3β (BD Transduction Labs; 610202), anti-phospho-Ser240/244 S6 ribosomal protein (Cell Signaling Technology; no. 2215), anti-S6 ribosomal protein (Cell Signaling Technology; no. 2212), anti-phospho-Thr202/Tyr204 ERK1/2 (Cell Signaling Technology; no. 9101), anti-ERK1/2 (Cell Signaling Technology; no. 9101), anti-PTEN (Santa Cruz; sc-7974) and anti-mouse $pVHL(m)_{CT}$ antibody (Thoma *et al*, 2007a).

Cilia assays

Production of lentivirus expressing Cre, MEF infections, generation of *Vhlh* knockdown immortalised MEFs and cilia assays were performed as described (Thoma *et al*, 2007a). RPE-1 cells were infected with retroviruses (pLMP) expressing short hairpin RNA interference encoding non-silencing control hairpin (n.s) (Hergovich *et al*, 2006) or sequences against *AKT1* (Openbiosystems; RHS1764-9208187) or *PTEN* (Openbiosystems; RHS1764-9494281). Cells were selected with 4 μg/ml puromycin. Expression of a second hairpin was achieved by infection with lentiviruses (pCMV-nz) expressing a non-silencing control hairpin (n.s) or a hairpin against *VHL*. pCMV-nz was cloned from pCMV-GIN-Zeo (Openbiosystems) by removing the eGFP cassette. pCMV-GIN-Zeo was digested with Pci1 and Afe1 followed by blunting with mung bean nuclease. After separation of the fragments on an agarose gel the corresponding fragment was purified and religated to form pCMV-nz. Cloning of n.s and *VHL* short hairpins into pCMV-nz was performed as described (Hergovich *et al*, 2006). After infection, cells were selected with 0.5 mg/ml G418. LY294,002 (Sigma; 10 μM), RAD001 (Novartis; 100 nM), U0126 (Sigma; 10 μM), ERK inhibitor II (Calbiochem; 1 μM) were added for 70 min prior to stimulation with 0 or 10% FCS for 4 h.

Real-time PCR analysis

Total RNA was prepared from powdered tissue using the RNeasy Mini Kit (Qiagen) and cDNA was prepared using random hexanucleotide primers and Ready-to-go you-prime first-strand beads (GE Healthcare). Real-time PCR analysis of cDNA was conducted using Absolute SYBR Green (Abgene) and the following primer pairs: Glut-1 (5′-GCTTATGGGCTTCTCCAAACT-3′, 5′-GGTGACACCTCTCCCACATAC-3′), CA9 (5′-TGCTCCAAGTGTCTGCTCAG-3′, 5′-CAGGTGCATCCTCTTCACTGG-3′), Pgk-1 (5′-TGGAGCCAACTCCGTTGTC-3′, 5′-CAGGCATTCTCGACTTCTGGG-3′), Vegf-a (5′-CTTGTTCAGAGCGGAGAAAGC-3′, 5′-ACATCTGCAAGTACGTTCGTT-3′), BNip3 (5′-GACGAAGTAGCTCCAAGAGTTCTCA-3′, 5′-CTATTTCAGCTCTGTTGGTATCTTGTG-3′), Redd1 (5′-CAAGGCAAGAGCTGCCATAG-3′, 5′-CCGGTACTTAGCGTCAGGG-3′).

Supplementary data

Supplementary data are available at *The EMBO Journal* Online (http://www.embojournal.org).

Acknowledgements

We thank all members of our laboratory for discussions. We are particularly grateful to Peter Igarashi and Andreas Trumpp for providing *Ksp1.3-Cre* and $Pten^{fl/fl}$ mice, respectively. This study was supported by grants to IJF from the VHL Family Alliance and to WK from the Dr Josef Steiner Foundation and Swiss National Science Foundation.

References

Choyke PL, Glenn GM, Walther MM, Zbar B, Weiss GH, Alexander RB, Hayes WS, Long JP, Thakore KN, Linehan WM (1992) The natural history of renal lesions in von Hippel–Lindau disease: a serial CT study in 28 patients. *AJR Am J Roentgenol* **159:** 1229–1234

Cross DA, Alessi DR, Cohen P, Andjelkovich M, Hemmings BA (1995) Inhibition of glycogen synthase kinase-3 by insulin mediated by protein kinase B. *Nature* **378:** 785–789

Ding Q, Xia W, Liu JC, Yang JY, Lee DF, Xia J, Bartholomeusz G, Li Y, Pan Y, Li Z, Bargou RC, Qin J, Lai CC, Tsai FJ, Tsai CH, Hung MC (2005) Erk associates with and primes GSK-3beta for its inactivation resulting in upregulation of beta-catenin. *Mol Cell* **19:** 159–170

Frew IJ, Krek W (2007) Multitasking by pVHL in tumour suppression. *Curr Opin Cell Biol* **19:** 685–690

Haase VH, Glickman JN, Socolovsky M, Jaenisch R (2001) Vascular tumors in livers with targeted inactivation of the von Hippel–Lindau tumor suppressor. *Proc Natl Acad Sci USA* **98:** 1583–1588

Hergovich A, Lisztwan J, Barry R, Ballschmieter P, Krek W (2003) Regulation of microtubule stability by the von Hippel–Lindau tumour suppressor protein pVHL. *Nat Cell Biol* **5:** 64–70

Hergovich A, Lisztwan J, Thoma CR, Wirbelauer C, Barry RE, Krek W (2006) Priming-dependent phosphorylation and regulation of the tumor suppressor pVHL by glycogen synthase kinase 3. *Mol Cell Biol* **26:** 5784–5796

Horiguchi A, Oya M, Uchida A, Marumo K, Murai M (2003) Elevated Akt activation and its impact on clinicopathological features of renal cell carcinoma. *J Urol* **169:** 710–713

Kim WY, Kaelin WG (2004) Role of VHL gene mutation in human cancer. *J Clin Oncol* **22:** 4991–5004

Lesche R, Groszer M, Gao J, Wang Y, Messing A, Sun H, Liu X, Wu H (2002) Cre/loxP-mediated inactivation of the murine Pten tumor suppressor gene. *Genesis* **32:** 148–149

Lin F, Hiesberger T, Cordes K, Sinclair AM, Goldstein LS, Somlo S, Igarashi P (2003) Kidney-specific inactivation of the KIF3A subunit of kinesin-II inhibits renal ciliogenesis and produces polycystic kidney disease. *Proc Natl Acad Sci USA* **100:** 5286–5291

Lonser RR, Glenn GM, Walther M, Chew EY, Libutti SK, Linehan WM, Oldfield EH (2003) von Hippel–Lindau disease. *Lancet* **361:** 2059–2067

Ma W, Tessarollo L, Hong SB, Baba M, Southon E, Back TC, Spence S, Lobe CG, Sharma N, Maher GW, Pack S, Vortmeyer AO, Guo C, Zbar B, Schmidt LS (2003) Hepatic vascular tumors, angiectasis in multiple organs, and impaired spermatogenesis in mice with conditional inactivation of the VHL gene. *Cancer Res* **63:** 5320–5328

Mandriota SJ, Turner KJ, Davies DR, Murray PG, Morgan NV, Sowter HM, Wykoff CC, Maher ER, Harris AL, Ratcliffe PJ, Maxwell PH (2002) HIF activation identifies early lesions in VHL kidneys: evidence for site-specific tumor suppressor function in the nephron. *Cancer Cell* **1:** 459–468

Nauli SM, Zhou J (2004) Polycystins and mechanosensation in renal and nodal cilia. *Bioessays* **26:** 844–856

Ophascharoensuk V, Giachelli CM, Gordon K, Hughes J, Pichler R, Brown P, Liaw L, Schmidt R, Shankland SJ, Alpers CE, Couser WG, Johnson RJ (1999) Obstructive uropathy in the mouse: role of osteopontin in interstitial fibrosis and apoptosis. *Kidney Int* **56:** 571–580

Pan J, Wang Q, Snell WJ (2005) Cilium-generated signaling and cilia-related disorders. *Lab Invest* **85:** 452–463

Pantuck AJ, Seligson DB, Klatte T, Yu H, Leppert JT, Moore L, O'Toole T, Gibbons J, Belldegrun AS, Figlin RA (2007) Prognostic relevance of the mTOR pathway in renal cell carcinoma: implications for molecular patient selection for targeted therapy. *Cancer* **109:** 2257–2267

Pastorekova S, Zavadova Z, Kostal M, Babusikova O, Zavada J (1992) A novel quasi-viral agent, MaTu, is a two-component system. *Virology* **187:** 620–626

Peters CA (2001) Animal models of fetal renal disease. *Prenat Diagn* **21:** 917–923

Pollard PJ, Spencer-Dene B, Shukla D, Howarth K, Nye E, El-Bahrawy M, Deheragoda M, Joannou M, McDonald S, Martin A, Igarashi P, Varsani-Brown S, Rosewell I, Poulsom R, Maxwell P, Stamp GW, Tomlinson IP (2007) Targeted inactivation of fh1 causes proliferative renal cyst development and activation of the hypoxia pathway. *Cancer Cell* **11:** 311–319

Rankin EB, Tomaszewski JE, Haase VH (2006) Renal cyst development in mice with conditional inactivation of the von Hippel–Lindau tumor suppressor. *Cancer Res* **66:** 2576–2583

Shao X, Somlo S, Igarashi P (2002) Epithelial-specific Cre/lox recombination in the developing kidney and genitourinary tract. *J Am Soc Nephrol* **13:** 1837–1846

Shin Lee J, Seok Kim H, Bok Kim Y, Cheol Lee M, Soo Park C (2003) Expression of PTEN in renal cell carcinoma and its relation to tumor behavior and growth. *J Surg Oncol* **84:** 166–172

Solomon D, Schwartz A (1988) Renal pathology in von Hippel–Lindau disease. *Hum Pathol* **19:** 1072–1079

Thoma CR, Frew IJ, Hoerner CR, Montani M, Moch H, Krek W (2007a) pVHL and GSK3beta are components of a primary ciliium-maintenance signalling network. *Nat Cell Biol* **9:** 588–595

Thoma CR, Frew IJ, Krek W (2007b) The VHL tumor suppressor: riding tandem with GSK3beta in primary cilium maintenance. *Cell Cycle* **6:** 1809–1813

Tsuruta H, Kishimoto H, Sasaki T, Horie Y, Natsui M, Shibata Y, Hamada K, Yajima N, Kawahara K, Sasaki M, Tsuchiya N, Enomoto K, Mak TW, Nakano T, Habuchi T, Suzuki A (2006) Hyperplasia and carcinomas in Pten-deficient mice and reduced PTEN protein in human bladder cancer patients. *Cancer Res* **66:** 8389–8396

Velickovic M, Delahunt B, McIver B, Grebe SK (2002) Intragenic PTEN/MMAC1 loss of heterozygosity in conventional (clear-cell) renal cell carcinoma is associated with poor patient prognosis. *Mod Pathol* **15:** 479–485

Yang H, Minamishima YA, Yan Q, Schlisio S, Ebert BL, Zhang X, Zhang L, Kim WY, Olumi AF, Kaelin Jr WG (2007) pVHL acts as an adaptor to promote the inhibitory phosphorylation of the NF-kappaB agonist Card9 by CK2. *Mol Cell* **28:** 15–27

Yoo LI, Liu DW, Le Vu S, Bronson RT, Wu H, Yuan J (2006) Pten deficiency activates distinct downstream signaling pathways in a tissue-specific manner. *Cancer Res* **66:** 1929–1939

Zhang HH, Lipovsky AI, Dibble CC, Sahin M, Manning BD (2006) S6K1 regulates GSK3 under conditions of mTOR-dependent feedback inhibition of Akt. *Mol Cell* **24:** 185–197